Important Notice to Authors

No further publication processing will occur until we receive your response to this proof.

Attached is a PDF proof of your forthcoming article in *Physical Review Letters*. The article accession code is LQ17413.

Your paper will be in the following section of the journal: LETTERS — Atomic, Molecular, and Optical Physics

Please note that as part of the production process, APS converts all articles, regardless of their original source, into standardized XML that in turn is used to create the PDF and online versions of the article as well as to populate third-party systems such as Portico, Crossref, and Web of Science. We share our authors' high expectations for the fidelity of the conversion into XML and for the accuracy and appearance of the final, formatted PDF. This process works exceptionally well for the vast majority of articles; however, please check carefully all key elements of your PDF proof, particularly any equations or tables.

Figures submitted electronically as separate files containing color appear in color in the online journal.
However, all figures will appear as grayscale images in the print journal unless the color figure charges have been paid in advance, in accordance with our policy for color in print (https://journals.aps.org/authors/color-figures-print).

Specific Questions and Comments to Address for This Paper

The numbered items below correspond to numbers in the margin of the proof pages pinpointing the source of the question and/or comment. The numbers will be removed from the margins prior to publication.

1 Except for the term "and/or," the use of the slash is discouraged between words and abbreviations, as the intent of the solidus is ambiguous. Several possibilities for its meaning exist, among them "and," "or," "and/or," and "plus." We ask that more precise, and therefore more meaningful, conjunctions be used. For terms that are diagrammatically opposed, we use a hyphen (e.g., liquid-solid interface, vacancy-acceptor interface).

2 It is journal style to break down fractions in superscripts and subscripts. Please check that fractions and added bracketing in Eqs. (6),(7),(9) appear acceptably.

3 Please write out FWM. Was FWHM intended?

4 Please review the funding information section of the proof's cover letter and respond as appropriate. We must receive confirmation that the funding agencies have been properly identified before the article can publish.

5 NOTE: External links, which appear as blue text in the reference section, are created for any reference where a Digital Object Identifier (DOI) can be found. Please confirm that the links created in this PDF proof, which can be checked by clicking on the blue text, direct the reader to the correct references online. If there is an error, correct the information in the reference or supply the correct DOI for the reference. If no correction can be made or the correct DOI cannot be supplied, the link will be removed.

6 A check of online databases revealed a possible error in Ref. [30]. The year has been changed from '2016' to '2017'. Please confirm this is correct.

Titles in References

The editors now encourage insertion of article titles in references to journal articles and e-prints. This format is optional, but if chosen, authors should provide titles for *all* eligible references. If article titles remain missing from eligible references, the production team will remove the existing titles at final proof stage.

ORCIDs

Please follow any ORCID links (iD) after the authors' names and verify that they point to the appropriate record for each author.

Funding Information

Information about an article's funding sources is now submitted to Crossref to help you comply with current or future funding agency mandates. Crossref's Open Funder Registry (https://www.crossref.org/services/funder-registry/) is the definitive registry of funding agencies. Please ensure that your acknowledgments include all sources of funding for your article following any requirements of your funding sources. Where possible, please include grant and award ids. Please carefully check the following funder information we have already extracted from your article and ensure its accuracy and completeness:

- Ministry of Education - Singapore, FundRef ID http://dx.doi.org/10.13039/501100001459 (Republic of Singapore/SG)

Other Items to Check

- Please note that the original manuscript has been converted to XML prior to the creation of the PDF proof, as described above. Please carefully check all key elements of the paper, particularly the equations and tabular data.
- Title: Please check; be mindful that the title may have been changed during the peer-review process.
- Author list: Please make sure all authors are presented, in the appropriate order, and that all names are spelled correctly.
- Please make sure you have inserted a byline footnote containing the email address for the corresponding author, if desired. Please note that this is not inserted automatically by this journal.
- Affiliations: Please check to be sure the institution names are spelled correctly and attributed to the appropriate author(s).
- Receipt date: Please confirm accuracy.
- Acknowledgments: Please be sure to appropriately acknowledge all funding sources.
- References: Please check to ensure that titles are given as appropriate.
- Hyphenation: Please note hyphens may have been inserted in word pairs that function as adjectives when they occur before a noun, as in “x-ray diffraction,” “4-mm-long gas cell,” and “*R*-matrix theory.” However, hyphens are deleted from word pairs when they are not used as adjectives before nouns, as in “emission by x rays,” “was 4 mm in length,” and “the *R* matrix is tested.”
  Note also that Physical Review follows U.S. English guidelines in that hyphens are not used after prefixes or before suffixes: superresolution, quasiequilibrium, nanoprecipitates, resonancelike, clockwise.
- Please check that your figures are accurate and sized properly. Make sure all labeling is sufficiently legible. Figure quality in this proof is representative of the quality to be used in the online journal. To achieve manageable file size for online delivery, some compression and downsampling of figures may have occurred. Fine details may have become somewhat fuzzy, especially in color figures. The print journal uses files of higher resolution and therefore details may be sharper in print. Figures to be published in color online will appear in color on these proofs if viewed on a color monitor or printed on a color printer.
- Overall, please proofread the entire *formatted* article very carefully. The redlined PDF should be used as a guide to see changes that were made during copyediting. However, note that some changes to math and/or layout may not be indicated.

Ways to Respond

- ***Web:*** If you accessed this proof online, follow the instructions on the web page to submit corrections.
- ***Email:*** Send corrections to aps-robot@luminad.com. Include the accession code LQ17413 in the subject line.
- ***Fax:*** Return this proof with corrections to +1.855.808.3897.

If You Need to Call Us

You may leave a voicemail message at +1.855.808.3897. Please reference the accession code and the first author of your article in your voicemail message. We will respond to you via email.

Spectral Compression of Narrowband Single Photons with a Resonant Cavity

Mathias A. Seidler,[1] Xi Jie Yeo,[2] Alessandro Cerè,[1] and Christian Kurtsiefer[1,2,*]
[1]Centre for Quantum Technologies, National University of Singapore, 3 Science Drive 2, Singapore 117543
[2]Department of Physics, National University of Singapore, 2 Science Drive 3, Singapore 117551

(Received 19 March 2020; accepted 7 October 2020)

We experimentally demonstrate a spectral compression scheme for heralded single photons with narrow spectral bandwidth around 795 nm, generated through four-wave mixing in a cloud of cold ^{87}Rb atoms. The scheme is based on an asymmetric cavity as a dispersion medium and a simple binary phase modulator, and can be, in principle, without any optical losses. We observe a compression from 20.6 MHz to less than 8 MHz, almost matching the corresponding atomic transition.

DOI:

Introduction.—Efficient atom-light interactions at the single quantum level is at the core of several proposals for storing, processing, and relaying quantum information [1–4]. Many of these schemes require single "flying" photons to match the spectrum of atomic transitions [5–8]. Single photons can be emitted from trapped ions [9,10], atoms [11–13], or solid-state systems [14–16]. However, the spectral width of the generated photons may not always match the spectral width of the receiving systems. Therefore, methods to engineer the photon spectrum may be required.

The simplest method for this is to passively filter the spectrum of bright broadband sources [17,18], with a sometimes significant reduction of brightness, making photon-atom interaction experiments that require a high interaction rate [19,20] difficult. More advanced methods to manipulate the spectrum of single photon sources to match that of atomic transitions include restricting the spectral mode of emitters with cavities [11,16,21,22], or using electromagnetically induced transparency in atomic ensembles [23,24] in the source mechanism altogether. As spectral filtering or engineering of the photon generation mechanism may not always be possible, it would be desirable to modify the spectrum of a given photon source while maintaining the brightness. To our knowledge, the only experiments to modify the photon spectrum of narrowband single photons use gradient echo quantum memories [25,26]. However, this was only demonstrated for photons with spectral bandwidths narrower than atomic absorption linewidths.

Here, we demonstrate an alternative technique that compresses the spectral bandwidth of single photons with a spectral bandwidth a few times broader than the corresponding atomic absorption linewidth, while in principle, maintaining the photon rates. The technique is based on the ideas of time lenses invented for temporal imaging [27,28], where the temporal and spectral characteristics of ultrafast electromagnetic pulses [29–31] are manipulated. It turns out that single photon states can be manipulated in a similar way, complementing the techniques for lossless temporal envelope manipulation of narrowband single photon states demonstrated in [32,33].

Spectral compression of single photon wave packets is achieved in two steps. First, the wave packet is spread out in time such that the width of its envelope is compatible with a narrow spectrum; this can be done using a dispersive element that spreads out different frequency components of the wave packet in time, effectively generating a chirped wave packet. In the second step, a time-dependent phase shift is applied. This step changes the spectral energy distribution of the wave packet.

Previous time-lens-based spectral compression schemes were performed on ultrashort pulses, using optical fibers or diffraction gratings as dispersive elements [29–31]. The suitability of a dispersive element for a spectral compression scheme is related to the spectral bandwidth of the optical pulse. The bandwidths of the ultrashort pulses used in previous time-lens-based spectral compression schemes are typically on the order of $0.1, \ldots, 1$ THz, and the length of optical fibers used to generate a significant temporal broadening of these pulses are on the order of $0.1, \ldots, 10$ km. However, photonic wave packets interacting with single emitters like atoms or molecules have spectral bandwidths on the order of MHz, which would require optical fibers on the order of 10^8 m to generate a suitable temporal broadening for spectral compression. Transmitting light through such a long fiber would not only be impractical, but also prohibitively lossy. Similarly, currently available gratings would not be able to significantly disperse photonic wave packets with bandwidths of a few MHz. We overcome this problem by using the dispersive properties of an optical cavity instead. While the dispersion in optical cavities can be much larger, the process then requires a different time-dependent phase shift in the second step to complete the spectral compression process.

Theory.—To understand the spectral compression scheme, we start with an initial single photon wave packet, described by an envelope $|\psi(t)|^2$ of its intensity in time, and its corresponding power spectrum $|\Psi(\omega;\omega_0,\Gamma_p)|^2$, connected by the Fourier transform F: $\Psi(\omega) = F[\psi(t)]$. The nearly monochromatic wave packet shall be characterized by a central frequency ω_0 and a spectral width Γ_p. The spreading out of the wave packet in time is accomplished by reflection off an asymmetric cavity, with an input-output coupler with a low transmission, and a second high-reflective mirror, similar to the setup used in [34].

If the losses in the cavity are negligible compared to the transmission of the coupling mirror, and the cavity linewidth Γ_c and photon bandwidth Γ_p are much smaller than free spectral range of the cavity, the action of the cavity to a wave packet near its resonance ω_c can be described by a transfer function

$$C(\omega;\omega_c,\Gamma_c) \approx -\frac{\Gamma_c + i2(\omega-\omega_c)}{\Gamma_c - i2(\omega-\omega_c)}, \qquad (1)$$

which modifies the incoming spectral wave packet $\Psi(\omega;\omega_0,\Gamma_p)$ to a new one,

$$\Psi'(\omega;\Delta\omega,\Gamma_c,\Gamma_p) = \Psi(\omega;\omega_0,\Gamma_p)C(\omega;\omega_c,\Gamma_c), \quad (2)$$

where $\Delta\omega = \omega_0 - \omega_c$ is the detuning between the wave packet and the cavity resonance. For a lossless cavity, this wave packet has the same power spectrum as $\Psi(\omega)$ because $|C(\omega;\omega_c,\Gamma_c)|^2 = 1$. The temporal envelope of the reflected wave packet, obtained through the inverse Fourier transform F^{-1},

$$\psi'(t;\Delta\omega,\Gamma_c,\Gamma_p) = F^{-1}[\Psi'(\omega;\Delta\omega,\Gamma_c,\Gamma_p)], \qquad (3)$$

is now broader in time, and has acquired a time-dependent phase $\phi'(t;\Delta\omega,\Gamma_p,\Gamma_c)$.

Similar to Fourier-transform limited pulses, where the time-bandwidth product is minimized by a frequency-independent spectral phase, we can reduce the spectral bandwidth of the heralded single photon by removing any time-dependent phase. This is done by applying a time-dependent phase shift

$$\phi_e(t) = -\phi'(t;\Delta\omega,\Gamma_p,\Gamma_c), \qquad (4)$$

resulting in the spectrally compressed wave packet

$$\psi''(t;\Delta\omega,\Gamma_p,\Gamma_c) = \psi'(t;\Delta\omega,\Gamma_p,\Gamma_c)e^{i\phi_e(t)}. \qquad (5)$$

To quantify the compression, we compare the spectral widths before and after the compression obtained from the respective power spectrum $|\psi''(\omega;\Delta\omega,\Gamma_p,\Gamma_c)|^2$ obtained through a Fourier transform of Eq. (5).

We now consider the specific case of a heralded single photon emerging from an atomic cascade decay, where we intend to compress the idler photon (see inset of Fig. 2). Detection of a signal photon projects the field in the idler mode into the heralded state

$$\psi(t) = \sqrt{\Gamma_p}e^{-\Gamma_p/[2(t-t_0)]}\Theta(t-t_0), \qquad (6)$$

where t_0 and t are the detection times of the signal and idler photons, respectively. The exponential decay with the constant Γ_p is a characteristic of the spontaneous process, while the Heaviside step function Θ is a consequence of the well-defined time order of the cascade decay process. For simplicity, we set $t_0 = 0$.

This temporal profile corresponds to a Lorentzian power spectrum for the idler photons, and its bandwidth is described by the full width at half maximum Γ_p, which also corresponds to the spectral window containing 50% of the total pulse energy. However, the compressed spectrum $|F^{-1}[\psi''(t)]|^2$ has multiple maxima, and is distinctly different from distributions where the full width at half maximum naturally quantifies the bandwidth. Hence, we instead define bandwidth as the smallest spectral width containing 50% of the total pulse energy, as this definition of bandwidth is compatible for both a Lorentzian and a generic spectrum.

To obtain the optimal cavity parameters, we numerically minimize the bandwidth of the compressed photon spectrum. We find that the maximal compression is achieved by a resonant cavity $\Delta\omega = 0$ with a bandwidth of $\Gamma_c \approx \Gamma_p/4$. Under these conditions, the compressed single photon time envelope can be written as

$$\psi''(t) = e^{-i\phi'(t)}\sqrt{\Gamma_p}\frac{2\Gamma_c e^{-(\Gamma_c/2)t} - (\Gamma_p+\Gamma_c)e^{-(\Gamma_p/2)t}}{\Gamma_p - \Gamma_c}\Theta(t), \qquad (7)$$

with a phase function

$$\phi'(t) = \pi\Theta\left(t - 2\frac{\log(\frac{\Gamma_p+\Gamma_c}{2\Gamma_c})}{\Gamma_p-\Gamma_c}\right). \qquad (8)$$

This is a step function changing the phase by π, with the transition occurring at the minimum of the dispersed photon's temporal intensity profile. The narrowest bandwidth achievable with compression based on an asymmetric cavity with this strategy is $\sim 0.3\Gamma_p$; the temporal envelopes and power spectra shown in Fig. 1 correspond to this choice.

Experiment.—Details of the actual experiment are shown in Fig. 2. We generate the time-ordered photon pairs by four-wave mixing in a cold ensemble of ^{87}Rb atoms in a cascade level scheme [12]. Pump beams at 780 and 776 nm excite atoms from the $5S_{1/2}, F = 2$ ground level to the $5D_{3/2}, F = 3$ level via a two-photon transition. The 762 nm (signal) and 795 nm (idler) photon pairs emerge from a

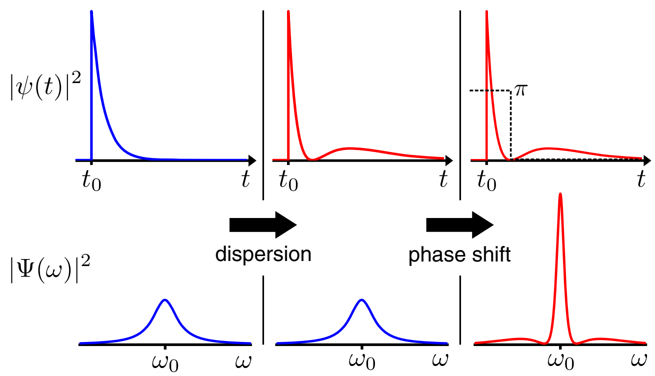

FIG. 1. Concept of spectral compression. The top row shows temporal intensity profiles $|\psi(t)|^2$ in various stages of the spectral compression, the bottom row the corresponding power spectra $|\Psi(\omega)|^2$. The initial pulse is dispersed by a cavity, leading to a new temporal shape, but an unchanged spectrum. An electro-optical modulator (EOM) manipulates the phase $\phi'(t)$ of the pulse which leads to a narrower spectrum.

cascade decay back to the ground level, and are coupled to single mode fibers. Phase matching is ensured with all four modes propagating collinearly in the same direction. The two pumps have a focus in the cloud with a beam waist of about 400 μm. The 780 nm pump is 55 MHz blue detuned from the $5S_{1/2}, F = 2$ to $5P_{3/2}, F = 3$ transition and has an optical power of 0.25 mW. The 776 nm pump has an optical power of 11.4 mW, and is tuned such that the two-photon transition to the $5D_{3/2}, F = 3$ state is 5 MHz blue detuned. When the excited atoms decay via the $5D_{1/2}, F = 2$ state back into the initial ground state, photons with a wavelength of 762 nm and 795 nm photon are emitted [12].

After suppressing residual pump light and separating signal and idler photons into different modes, we collect them into single mode fibers. The 762 nm signal photons are detected with an avalanche photo diode and herald the presence of 795 nm idler photons. The time correlation between the detection in the signal and idler modes (open circles in Fig. 3) correspond to the envelope $|\psi(t)|^2$ of the intensity in time.

We measure the initial power spectrum of the wave packet (open circles in Fig. 4) by correlating it with a the photon rate transmitted through a Fabry-Perot cavity (FP) with linewidth $\Gamma_{\mathrm{FP}} \approx 2\pi \times 2.6$ MHz. The transmission is recorded at different detunings of the cavity from the atomic resonance. The observed spectrum was observed to have a full width at half maximum of 20(2) MHz, wider than the atomic linewidth of 6 MHz due to collective emission effects in the cloud [35,36].

The 795 nm idler photons are then coupled to the dispersion cavity, with a coupling mirror of nominal reflectivity $R_1 = 0.97$, and a high reflector with $R_2 = 0.9995$ separated by 10.1 cm, corresponding to a free spectral range of 1.48 GHz, and a measured linewidth $\Gamma_c \approx 2\pi \times 7.3$ MHz. A Pound-Drever-Hall frequency lock keeps the cavity resonant to the central frequency of the photons throughout the experiment. The measured time envelope of the single photon wave packet after dispersion is shown as filled dots in Fig. 3.

The spectral compression is completed by applying the temporal phase of Eq. (8), in the form of a phase switch synchronized to the photon passage through a fiber connected electro-optical modulator (EOM). Since the idler photon is heralded, we use the detection of the signal photon as a reference signal for triggering the phase switch

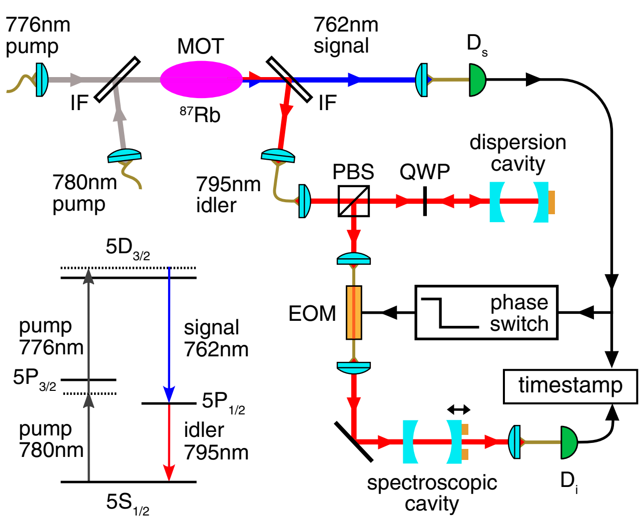

FIG. 2. Schematic setup for generation and spectral compression of heralded single photons. $D_{S,I}$: single-photon detectors; EOM: electro-optical modulator; PBS: polarizing beam splitter; QWP: quarter-wave plate; IF: interference filter. Inset: energy level scheme for four-wave mixing in ^{87}Rb.

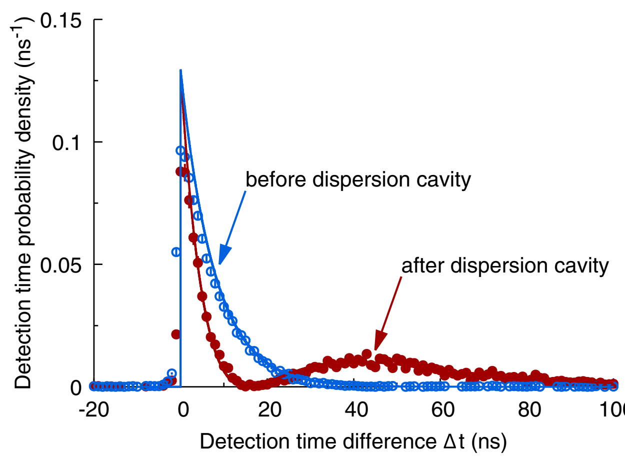

FIG. 3. Detection time distribution for the heralded photon before (open blue circles) and after (filled red dots) the dispersion cavity. We fit an exponential decay Eq. (6) to the initial time correlation (blue solid line), from which we infer the photon bandwidth Γ_p. The simulated temporal profile after the photon passed through the dispersion cavity [red line, calculated from Eq. (2)], matches our experimental data (filled dots) well.

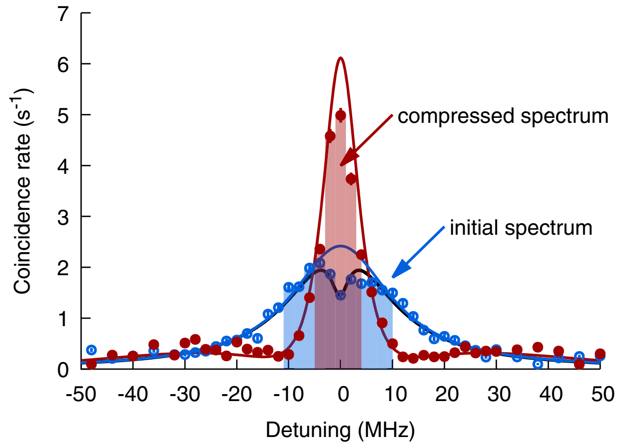

FIG. 4. Spectral profile of heralded photons before (blue) and after (red) spectral compression, obtained by measuring the photon transmission rate through the Fabry-Perot cavity at different cavity detunings. The solid lines are calculated from Eq. (5), with Γ_p inferred from the temporal envelope measurement of the photons from the source, and Γ_c by experimentally characterizing the cavity bandwidth. Shaded areas cover 50% of the total power for each spectrum.

after an appropriate time delay. Our dispersed photon is approximately 80 ns long, which corresponds to a spatial spread of 16 m in a fiber with a refractive index of 1.5. The phase modulator has an active length of 90 mm, so at any instant only a small part of the photon resides inside the EOM, and we are able to modulate the two parts of the photon with different phases. The correct timing of the phase modulation is ensured by measuring the length of the fibers and the electric signal lines with a timing uncertainty < 0.5 ns, on par with the electrical rise time of the phase change signal. This order of timing uncertainty can be tolerated, since the majority of second photon wave packet part (Fig. 3, blue line from 15 to 100 ns) gets a phase shift of π. The phase flip is applied right after the first part of the dispersed photon exits the modulator, and the second part starts to propagate through it. This timing is indicated as the dashed line in Fig. 1. We finally measure the compressed photon spectrum by again recording the photon transmission rate through the Fabry-Perot cavity, shown as filled dots in Fig. 4.

To obtain an initial photon bandwidth Γ_p, we fit the decaying exponential term in Eq. (6) to the observed coincidence probability (open circles in Fig. 3). The solid red line in Fig. 3 corresponds to an expected temporal profile of the photon after the dispersion cavity, calculated from Eq. (7), with an inferred photon bandwidth $\Gamma_p = 2\pi \times 20.6(2)$ MHz obtained from the fit of the initial photon shape, and the cavity linewidth $\Gamma_c \approx 2\pi \times 7.3$ MHz measured earlier. The observed temporal envelope after the dispersion cavity (full dots in Fig. 3) agrees very well with the expected profile.

The measured spectral profiles before and after compression are shown in Fig. 4. The spectrum of the uncompressed photons (open circles) exhibits a dip around the central frequency, which was also observed without the compression optics. We attribute this to reabsorption of the generated photons by the atomic cloud. We model this spectrum $S(\omega)$ by considering two processes: First, we consider the spectrum $P(\omega)$ of the photon emitted by the atomic cloud which can be obtained by the product of the spectrum of the photon produced by our FWM process $L(\omega;\Gamma_p) = (2/\pi)(\Gamma_p/4\omega^2 + \Gamma_p^2)$ and an absorption term describing the attenuation of the photon by our atomic cloud of optical density OD

$$P(\omega;\mathrm{OD},\Gamma_p,\Gamma_a) = AL(\omega;\Gamma_p)e^{-\mathrm{OD}[\Gamma_a^2/(4\omega^2+\Gamma_a^2)]}. \quad (9)$$

The scaling factor A is used to account for the detected coincidence rate, and Γ_a is the spectral width of the absorption feature. From our fit, we extract $\Gamma_a = 2\pi \times 1.38(1.6)$ MHz, which does not correspond to the absorption linewidth of the corresponding atomic linewidth ($2\pi \times 5.7$ MHz) of the $5S_{1/2} \to 5P_{1/2}$ transition. Further work is necessary to understand this observation. The inferred photon bandwidth $\Gamma_p = 2\pi \times 20.6(2)$ MHz was determined from the photon coincidence time correlation (Fig. 3). Second, we consider the effect of the Fabry-Perot cavity used to sample the spectral profile by convolution the above result with $L'(\omega;\Gamma_{\mathrm{FP}}) = [\Gamma_{\mathrm{FP}}^2/(4\omega^2 + \Gamma_{\mathrm{FP}}^2)]$ to model the observed spectrum:

$$S(\omega) = (P * L')(\omega). \quad (10)$$

We fit the model $S(\omega)$ (Fig. 4, black line) to the experimental data corresponding to the spectral profile of the photon without sending a signal to the EOM used to compress the photon. The model, without considering the attenuation of the atomic cloud, is given by $(AL * L')(\omega)$ (Fig. 4, blue line). This is provided as a reference for a Fourier-transform limited photon with an exponentially decaying envelope, as emitted by a single atom—the scenario examined in the theory section.

To apply the analysis in the theory section for predicting the spectrum of the compressed photon, we first rescale the power spectrum $|\Psi''(\omega)|^2$, calculated from Eq. (7), with A, which was extracted from the previous fit. Then, we convolve this spectrum with $L'(\omega;\Gamma_{\mathrm{FP}})$ to obtain the expected compressed photon spectrum $(A|\Psi''|^2 * L')(\omega)$. Figure 4 (red line) shows the modeled power spectrum slightly deviating from the measured result (red dots), exhibiting a lower peak coincidence rate where an absorption dip occurs in the uncompressed photon spectrum (blue dots). We attribute this difference to the fact that our model does not fully account for the effects imposed by the atomic cloud.

Discussion.—By definition, spectral compression reduces the width of a spectral distribution, resulting in an increased photon rate and intensity at the central frequency. In our experiment, we observed a bandwidth of 20(2) MHz for the initial photon, and 8(2) MHz for the compressed photon from spectroscopy using a 2.6 MHz cavity. This almost matches the natural D transition linewidth of 6 MHz in ^{87}Rb. The maximal photon transmission through the spectroscopic cavity is increased by a factor of 2.39(4), indicating a successful spectral compression of narrowband photons.

The compressions mechanism is, in principle, lossless since both cavity and phase modulators can have arbitrarily low losses. In our experiment, however, we observe an overall transmission of 22% through the compression optics; the dispersion optics alone (PBS, QWP, dispersion cavity) has a transmission of 72%, and the fiber-based EOM a transmission of 30% including the fiber coupling.

To compare the compression method with simple passive filtering, we calculate the transmission T of the 20 MHz bandwidth photons produced by our source through both bandwidth-limiting schemes, and an analyzer cavity with a bandwidth of 6 MHz bandwidth and resonant with the central frequency of the input photons to model an atomic absorption process corresponding to the $5S_{1/2} \rightarrow 5P_{1/2}$ transition in ^{87}Rb. With a lossless compression system, we find $T = 44\%$, while a resonant filter cavity of the same bandwidth of 6 MHz leads to $T = 14\%$, illustrating the advantage of the compression method. By replacing the fiber-based EOM with a free-space EOM with an optical transmission $> 95\%$, the compression method would significantly surpass the transmission of a passive filter.

Optimal spectral compression of a photon with bandwidth Γ_p in the cavity-based scheme is achieved if the dispersion cavity has a bandwidth of $0.25\Gamma_p$. Since the amount of spectral compression is limited by the dispersion mechanism, dispersion engineering of structured dielectric media [37–39] or multiple combined optical cavities may allow us to further increase the spectral compression. This method is not limited to the atomic system in our experiment—it can be adapted to a wide range of wavelengths and spectral widths, and therefore even allow us to match the spectral properties to different types of quantum systems, e.g., in a hybrid quantum network [40].

We thank Adrian Nugraha Utama for useful discussions on the theoretical modeling and Jianwei Lee for his valuable input while writing this script. This work was supported by the Ministry of Education in Singapore.

*christian.kurtsiefer@gmail.com

[1] J. I. Cirac, P. Zoller, H. J. Kimble, and H. Mabuchi, Phys. Rev. Lett. **78**, 3221 (1997).

[2] H.-J. Briegel, W. Dür, J. I. Cirac, and P. Zoller, Phys. Rev. Lett. **81**, 5932 (1998).

[3] E. Waks and C. Monroe, Phys. Rev. A **80**, 062330 (2009).

[4] H. J. Kimble, Nature (London) **453**, 1023 (2008).

[5] T. Wilk, S. C. Webster, A. Kuhn, and G. Rempe, Science **317**, 488 (2007).

[6] K. Hammerer, A. S. Sørensen, and E. S. Polzik, Rev. Mod. Phys. **82**, 1041 (2010).

[7] M. D. Lukin, Rev. Mod. Phys. **75**, 457 (2003).

[8] M. Steiner, V. Leong, M. A. Seidler, A. Cerè, and C. Kurtsiefer, Opt. Express **25**, 6294 (2017).

[9] M. Keller, B. Lange, K. Hayasaka, W. Lange, and H. Walther, Nature (London) **431**, 1075 (2004).

[10] M. Almendros, J. Huwer, N. Piro, F. Rohde, C. Schuck, M. Hennrich, F. Dubin, and J. Eschner, Phys. Rev. Lett. **103**, 213601 (2009).

[11] A. Kuhn, M. Hennrich, and G. Rempe, Phys. Rev. Lett. **89**, 067901 (2002).

[12] B. Srivathsan, G. K. Gulati, B. Chng, G. Maslennikov, D. N. Matsukevich, and C. Kurtsiefer, Phys. Rev. Lett. **111**, 123602 (2013).

[13] J. Park, H. Kim, and H. S. Moon, Phys. Rev. Lett. **122**, 143601 (2019).

[14] C. Kurtsiefer, S. Mayer, P. Zarda, and H. Weinfurter, Phys. Rev. Lett. **85**, 290 (2000).

[15] P. Michler, A. Kiraz, C. Becher, W. Schoenfeld, P. Petroff, L. Zhang, E. Hu, and A. Imamoglu, Science **290**, 2282 (2000).

[16] E. Moreau, I. Robert, J. Gérard, I. Abram, L. Manin, and V. Thierry-Mieg, Appl Phys. Lett. **79**, 2865 (2001).

[17] E. Meyer-Scott, N. Montaut, J. Tiedau, L. Sansoni, H. Herrmann, T. J. Bartley, and C. Silberhorn, Phys. Rev. A **95**, 061803(R) (2017).

[18] C. Schuck, F. Rohde, N. Piro, M. Almendros, J. Huwer, M. W. Mitchell, M. Hennrich, A. Haase, F. Dubin, and J. Eschner, Phys. Rev. A **81**, 011802(R) (2010).

[19] L.-M. Duan, M. D. Lukin, J. I. Cirac, and P. Zoller, Nature (London) **414**, 413 (2001).

[20] B. B. Blinov, D. L. Moehring, L.-M. Duan, and C. Monroe, Nature (London) **428**, 153 (2004).

[21] J. McKeever, A. Boca, A. D. Boozer, R. Miller, J. R. Buck, A. Kuzmich, and H. J. Kimble, Science **303**, 1992 (2004).

[22] F. Wolfgramm, X. Xing, A. Cerè, A. Predojević, A. M. Steinberg, and M. W. Mitchell, Opt. Express **16**, 18145 (2008).

[23] M. Eisaman, A. André, F. Massou, M. Fleischhauer, A. Zibrov, and M. Lukin, Nature (London) **438**, 837 (2005).

[24] L. Zhu, X. Guo, C. Shu, H. Jeong, and S. Du, Appl Phys. Lett. **110**, 161101 (2017).

[25] B. Buchler, M. Hosseini, G. Hétet, B. Sparkes, and P. K. Lam, Opt. Lett. **35**, 1091 (2010).

[26] B. M. Sparkes, M. Hosseini, C. Cairns, D. Higginbottom, G. T. Campbell, P. K. Lam, and B. C. Buchler, Phys. Rev. X **2**, 021011 (2012).

[27] B. H. Kolner and M. Nazarathy, Opt. Lett. **14**, 630 (1989).

[28] B. H. Kolner, IEEE J. Quantum Electron. **30**, 1951 (1994).

[29] J. Lavoie, J. M. Donohue, L. G. Wright, A. Fedrizzi, and K. J. Resch, Nat. Photonics **7**, 363 (2013).

[30] M. Karpiński, M. Jachura, L. J. Wright, and B. J. Smith, Nat. Photonics **11**, 53 (2017).

[31] Y. Li, T. Xiang, Y. Nie, M. Sang, and X. Chen, Sci. Rep. **7**, 43494 (2017).

[32] B. Srivathsan, G. K. Gulati, A. Cerè, B. Chng, and C. Kurtsiefer, Phys. Rev. Lett. **113**, 163601 (2014).

[33] O. Morin, M. Körber, S. Langenfeld, and G. Rempe, Phys. Rev. Lett. **123**, 133602 (2019).

[34] B. Srivathsan, G. K. Gulati, A. Cerè, B. Chng, and C. Kurtsiefer, Phys. Rev. Lett. **113**, 163601 (2014).

[35] H. H. Jen, Phys. Rev. A **85**, 013835 (2012).

[36] A. Cerè, B. Srivathsan, G. K. Gulati, B. Chng, and C. Kurtsiefer, Phys. Rev. A **98**, 023835 (2018).

[37] E. Istrate and E. H. Sargent, Rev. Mod. Phys. **78**, 455 (2006).

[38] X. Li, M. Pu, X. Ma, Y. Guo, P. Gao, and X. Luo, J. Phys. D **51**, 054002 (2018).

[39] J. D. Joannopoulos, S. G. Johnson, J. N. Winn, and R. D. Meade, *Photonic Crystals: Molding the Flow of Light*, 2nd ed. (Princeton University Press, Princeton, NJ, USA, 2008).

[40] G. Kurizki, P. Bertet, Y. Kubo, K. Mølmer, D. Petrosyan, P. Rabl, and J. Schmiedmayer, Proc. Natl. Acad. Sci. U.S.A. **112**, 3866 (2015).